AN ANALYTIC METHOD TO DETERMINE FUTURE CLOSE APPROACHES BETWEEN SATELLITES

FELIX R. HOOTS, LINDA L. CRAWFORD, and RONALD L. ROEHRICH
Hq NORAD/Space Command, Peterson Air Force Base, Colo., U.S.A.

(Received 23 December, 1983; accepted 25 January, 1984)

ABSTRACT. The calculation of the times of future close approaches between pairs of satellites has been formulated using analytical techniques. The resulting analytical equations are solved using numerical iterative techniques similar to solving Kepler's equation. A solution is obtained in a very efficient manner by use of a series of prefilters which eliminate many cases from further consideration. The method is valid for all values of eccentricities less than one and all relative geometries between the two orbits. This approach produces results in a very efficient and reliable manner.

1. INTRODUCTION

Because of the ever increasing number of objects in orbit about the Earth, the future prediction of close approaches between orbiting objects is becoming a routine requirement. This is necessary both for the safety of Shuttle crews as well as the protection of operational satellites from inadvertent collision. To protect or warn a satellite (called the primary) of a future collision, its orbit must be compared with every other object (called secondaries) in orbit about the Earth. Currently (November 1983) the total number of catalogued orbiting objects (payloads, rocket bodies, and debris) is almost 5000. Future warning for a primary may mean as much as a several day span in which all close encounters with each of the other 5000 secondaries are predicted.

The problem is stated most generally by specifying a time span of interest, say $[t_B, t_E]$, and a separation distance D. As two satellites move around their respective orbits, the relative separation distance between the two is given by

$$r_{rel} = |\underline{r}_p - \underline{r}_s|,$$

where $\underline{r}$ denotes the position vector of the satellite and where the subscripts p and s denote the primary and secondary satellite, respectively. Over the span of interest, a graph of r_{rel} might appear as in Figure 1. We seek all points of closest approach which are less than the threshold D (e.g., times t_1 and t_2 in Figure 1).

Since these points are simply relative minima of the function r_{rel}, the most obvious solution to the problem would be a numerical technique.

Celestial Mechanics **33** (1984) 143-158. 0008-8714/84/0332-0143 $02.40.

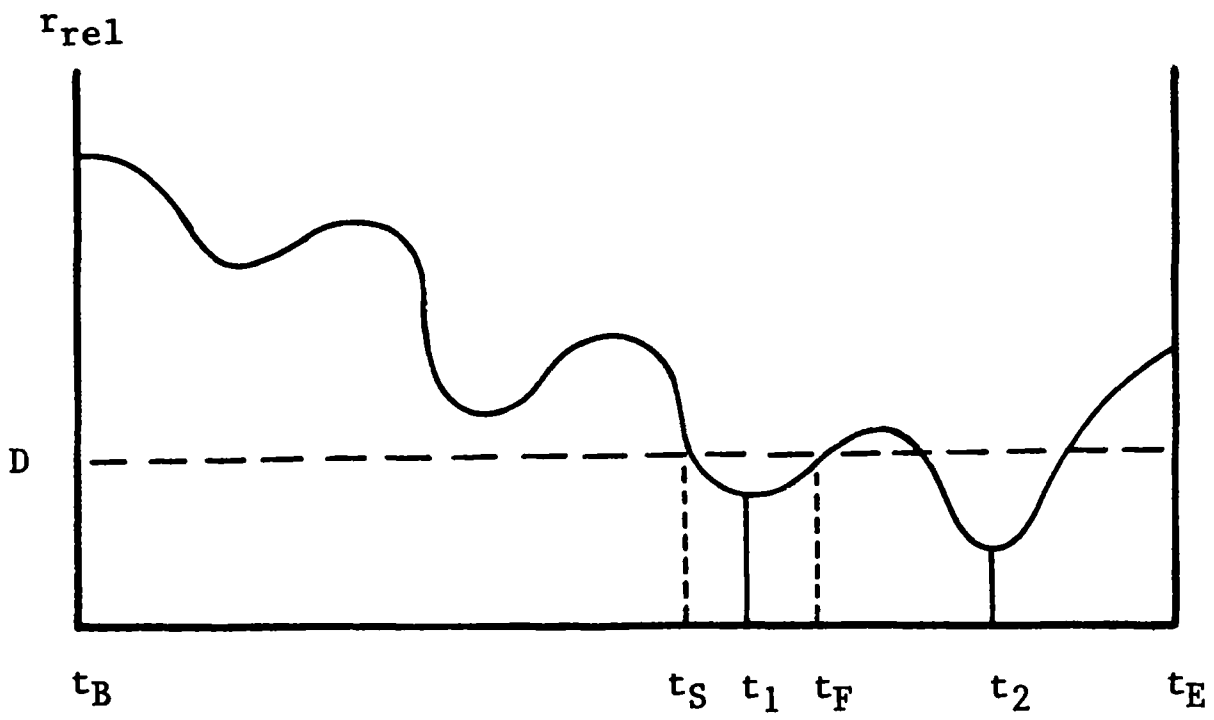

Fig. 1. Relative separation distance.

Starting at the beginning of the time interval of interest, we could numerically step along the primary and secondary orbits noting the relative separation distances. Whenever the relative distance changed from decreasing to increasing, we would know we had passed a relative minima. If this minima was less than D, we would record this time as a time of close approach. Stepping would continue until we reached the end of the time interval of interest. If we wanted to find all times of close approach with all orbiting objects, the procedure would be repeated for each of the 5000 secondaries. Clearly this procedure consumes exorbitant amounts of computer processing time. When we consider the task of collision alerting for many primaries, use of numerical techniques becomes hopeless.

Thus, to make the task manageable, we take an analytical approach to the solution. The general problem is broken down into the non-coplanar and the coplanar cases. In each case, a list of candidate times is produced by analytical equations. These candidates are generally very close to the exact times of close approach. They are refined by an iterative technique to produce the times of closest approach. Periods of close proximity when the two satellites are within the distance D are calculated in a similar way.

In the discussion which follows, it will first be assumed that the satellites follow two-body Keplerian orbits with no perturbations. The effect of perturbations on the candidate times is small and is easily incorporated as a minor modification to the analytical equations.

2. GEOMETRICAL PREFILTERS

Many of the possible secondaries can be eliminated from consideration because the relative geometry of the two ellipses does not allow the two trajectories to ever come within the threshold distance D. The simplest

test is a perigee-apogee test. Let q denote the larger of the two perigees and let Q denote the smaller of the two apogees. If

$$q - Q > D \tag{1}$$

then the secondary need not be considered further.

If a secondary is not eliminated by the perigee-apogee prefilter, then it is subjected to a second prefilter. This geometrical prefilter considers the relative geometry of the two ellipses in space. Figure 2 illustrates two arbitrary ellipses and the line of intersection of the two orbital planes.

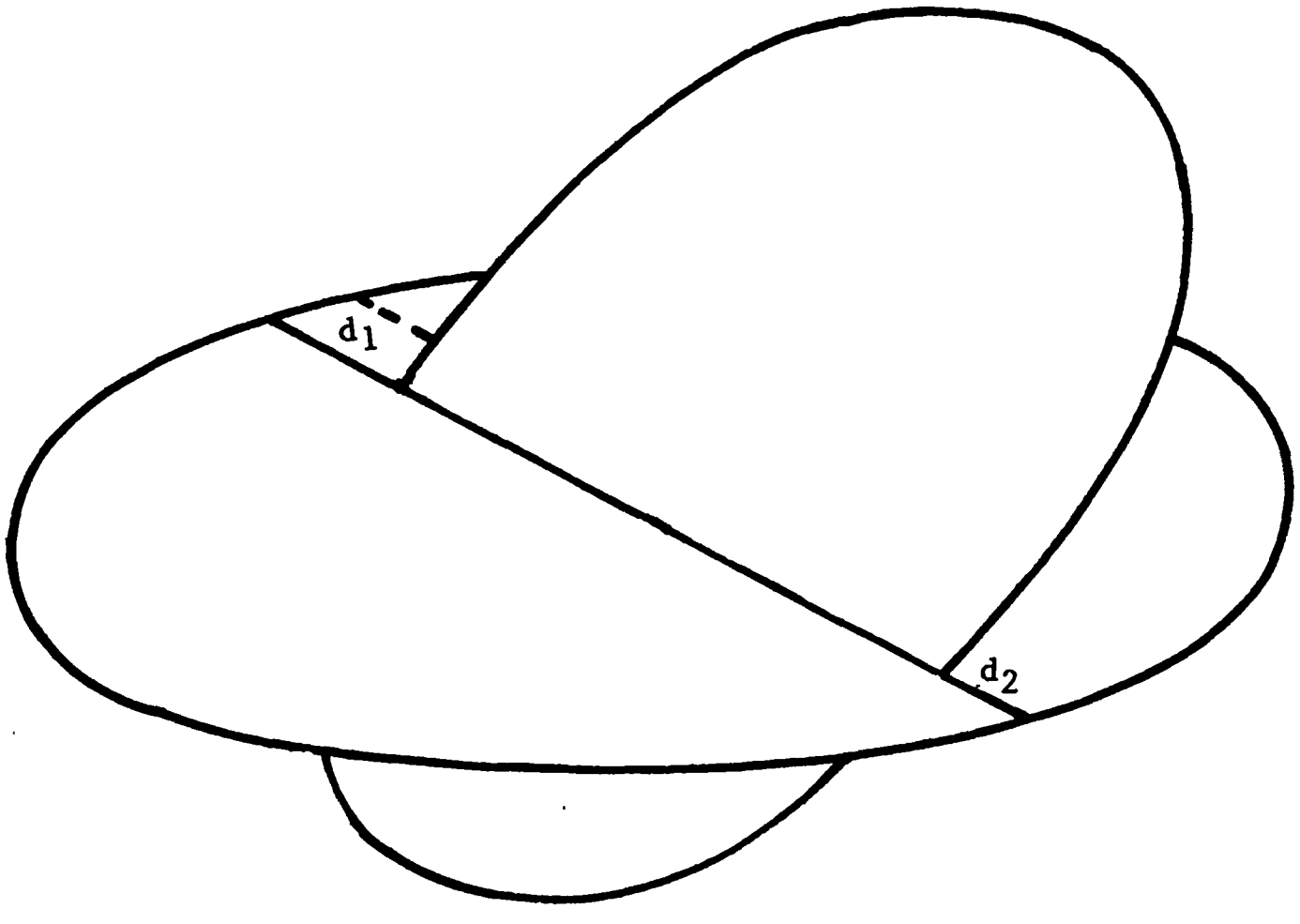

Fig. 2. Geometrical prefilter.

There will be two values d_1 and d_2 of closest approach distance between the two elliptical paths. It should be noted that the points are not necessarily along the line of intersection of the two planes. This is a purely geometrical calculation and is independent of the location of the two satellites on their elliptical paths. If the minimum distance in space between the two paths is greater than the separation distance D, then the satellites cannot have a close encounter of interest. Let

$$\underline{K} = \underline{w}_s \times \underline{w}_p, \tag{2}$$

where $\underline{w}_s$ and $\underline{w}_p$ are unit vectors normal to the orbital planes of the secondary and primary satellites, respectively, and where the underline denotes a vector. These unit vectors can be calculated with the equation

$$\underline{w} = \sin \Omega \sin I \, \underline{i} + \cos \Omega \sin I \, \underline{j} + \cos I \, \underline{k}, \tag{3}$$

where Ω is the longitude of ascending node, I is the inclination, and $\underline{i}$, $\underline{j}$, and $\underline{k}$ are unit vectors in the x, y, and z directions. The vector $\underline{K}$ lies along the line of intersection of the two orbital planes and has the additional property that

$$|\underline{K}| = \sin I_R, \tag{4}$$

where I_R is the relative inclination angle between the two orbital planes. It should be noted that, in general, I_R is not simply the difference between the inclinations of the two orbits. If I_R is identically zero, the geometrical prefilter equations become indeterminate and such cases must be treated by the coplanar method.

The orientation of the vector $\underline{K}$ within the orbital plane of either satellite is given by the angle Δ between the line of ascending node of the satellite plane and the vector $\underline{K}$ as illustrated in Figure 3. Let

$$\underline{n}_p = \cos \Omega_p \, \underline{i} + \sin \Omega_p \, \underline{j} \tag{5}$$

be a unit vector along the line of ascending node of the primary satellite. Then

$$\underline{K} \cdot \underline{n}_p = \sin I_p \cos I_s - \sin I_s \cos I_p \cos(\Omega_p - \Omega_s). \tag{6}$$

But from Figure 3, it is clear that

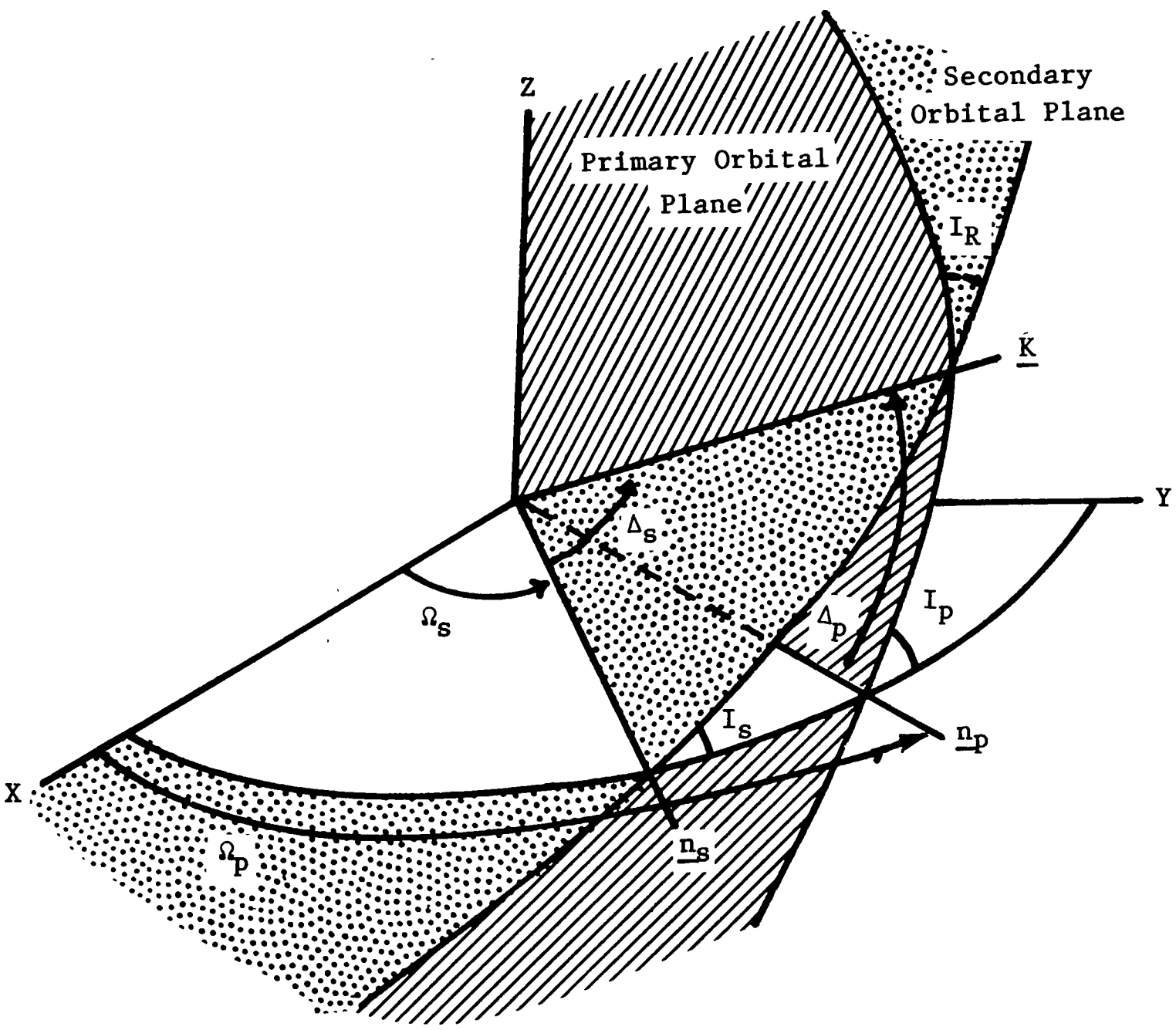

Fig. 3. Relative orientation of orbital planes.

$$\begin{aligned} \underline{K} \cdot \underline{n}_p &= |\underline{K}| \cos \Delta_p \\ &= \sin I_R \cos \Delta_p. \end{aligned} \tag{7}$$

Thus,

$$\cos \Delta_p = \frac{1}{\sin I_R} [\sin I_p \cos I_s - \sin I_s \cos I_p \cos(\Omega_p - \Omega_s)]. \tag{8}$$

Also, by using the law of sines in spherical trigonometry, we get

$$\sin \Delta_p = \frac{1}{\sin I_R} [\sin I_s \sin(\Omega_p - \Omega_s)]. \tag{9}$$

From Equations (8) and (9), Δ_p is uniquely determined. Similarly, it can be shown that

$$\cos \Delta_s = \frac{1}{\sin I_R} [\sin I_p \cos I_s \cos(\Omega_p - \Omega_s) - \sin I_s \cos I_p] \tag{10}$$

and

$$\sin \Delta_s = \frac{1}{\sin I_R} [\sin I_p \sin(\Omega_p - \Omega_s)]. \tag{11}$$

Let u_R denote the angle within the orbital plane from the vector $\underline{K}$ to the satellite position measured positive in the sense of the satellite motion as shown in Figure 4.

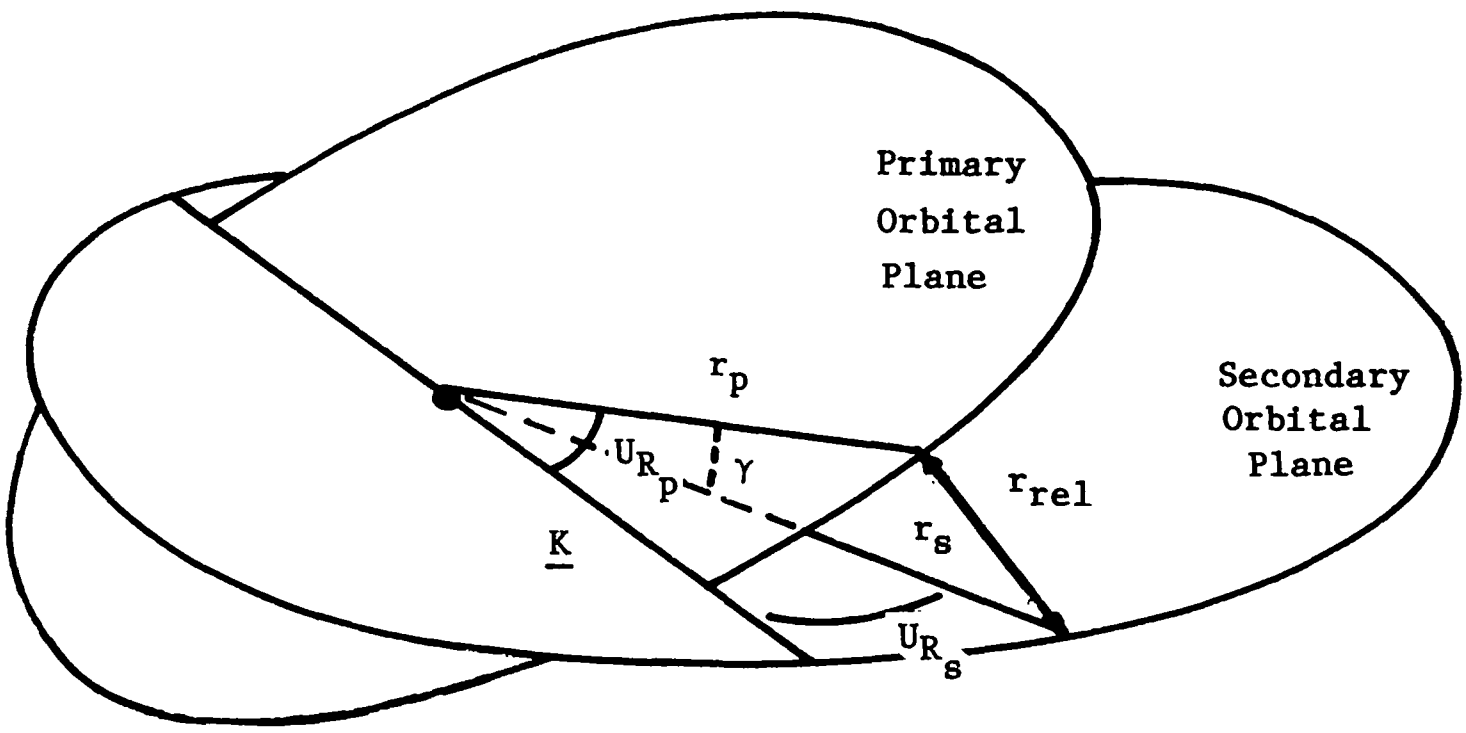

Fig. 4. Satellite positions in orbital planes.

Let r_p and r_s denote the magnitude of the position vectors of the primary and secondary satellites and let γ denote the angle between the two position vectors. Then

$$r_{rel}^2 = r_p^2 + r_s^2 - 2r_p r_s \cos \gamma. \tag{12}$$

From spherical trigonometry

$$\cos \gamma = \cos u_{R_p} \cos u_{R_s} + \sin u_{R_p} \sin u_{R_s} \cos I_R. \tag{13}$$

The point of closest approach of the two elliptical paths will be a relative minimum of the function in Equation (12). It is a function of the true anomalies of the two satellites since

$$u_R = f + \omega - \Delta, \tag{14}$$

where f is the true anomaly and ω is the argument of perigee. Thus, the relative minimum will be the solution of the two simultaneous equations

$$\frac{\partial r_{rel}^2}{\partial f_p} = 0, \quad \frac{\partial r_{rel}^2}{\partial f_s} = 0. \tag{15}$$

After considerable calculation and the use of Equations (13) and (14), Equations (15) reduce to

$$\begin{aligned} r_p e_p \sin f_p + r_s[&\cos u_{R_s}(\sin u_{R_p} + a_{y_p}) - \\ &- \sin u_{R_s} \cos I_R(\cos u_{R_p} + a_{x_p})] = 0, \\ r_s e_s \sin f_s + r_p[&\cos u_{R_p}(\sin u_{R_s} + a_{y_s}) - \\ &- \sin u_{R_p} \cos I_R(\cos u_{R_s} + a_{x_s})] = 0, \end{aligned} \tag{16}$$

where we have introduced the notation

$$a_x = e \cos(\omega - \Delta), \quad a_y = e \sin(\omega - \Delta). \tag{17}$$

For the case of two circular orbits, Equations (16) have the solution

$$f_p = \Delta_p - \omega_p, \quad f_s = \Delta_s - \omega_s. \tag{18}$$

For noncircular cases the analytical solution of Equations (16) seems intractable. However, the equations readily admit an iterative solution by Newton's method. Given equations of the form

$$F(f_p, f_s) = 0, \quad G(f_p, f_s) = 0. \tag{19}$$

Newton's method gives the iterative solution

$$f_{p_{i+1}} = f_{p_i} + h, \quad f_{s_{i+1}} = f_{s_i} + k, \tag{20}$$

where

$$h = \frac{F\dfrac{\partial G}{\partial f_s} - G\dfrac{\partial F}{\partial f_s}}{\dfrac{\partial F}{\partial f_s}\dfrac{\partial G}{\partial f_p} - \dfrac{\partial F}{\partial f_p}\dfrac{\partial G}{\partial f_s}}, \quad k = \frac{G\dfrac{\partial F}{\partial f_p} - F\dfrac{\partial G}{\partial f_p}}{\dfrac{\partial F}{\partial f_s}\dfrac{\partial G}{\partial f_p} - \dfrac{\partial F}{\partial f_p}\dfrac{\partial G}{\partial f_s}},$$

$$
\begin{aligned}
F &= r_p e_p \sin f_p + r_s(A \cos u_{R_s} - B \cos I_R \sin u_{R_s}), \\
G &= r_s e_s \sin f_s + r_p(C \cos u_{R_p} - D \cos I_R \sin u_{R_p}),
\end{aligned} \tag{21}
$$

$$
\frac{\partial F}{\partial f_p} = r_p e_p \cos E_p + r_s \cos \gamma,
$$

$$
\frac{\partial F}{\partial f_s} = - \frac{r_s}{1 + e_s \cos f_s} (AC + BD \cos I_R),
$$

$$
\frac{\partial G}{\partial f_p} = - \frac{r_p}{1 + e_p \cos f_p} (AC + BD \cos I_R),
$$

$$
\frac{\partial G}{\partial f_s} = r_s e_s \cos E_s + r_p \cos \gamma,
$$

with

$$
\begin{aligned}
A &= \sin u_{R_p} + a_{y_p}, \quad & C &= \sin u_{R_s} + a_{y_s}, \\
B &= \cos u_{R_p} + a_{x_p}, \quad & D &= \cos u_{R_s} + a_{x_s},
\end{aligned} \tag{22}
$$

and where E denotes the eccentric anomaly and cos γ is given by Equation (13). A starting value for the iteration is given by Equations (18). Let f_{p*} and f_{s*} denote the final converged values from the iteration. These are used in Equation (12) to calculate one point of closest approach between the two elliptical paths. There is another point of geometrical closeness which must be considered. It is found by iteration on Equations (16) using the starting values

$$
f_{p_1} = f_{p*} + \pi, \quad f_{s_1} = f_{s*} + \pi. \tag{23}
$$

The converged values from the iteration are used in Equation (12) to calculate the other point of closest approach between the two elliptical paths. If both points of closest approach are greater than D, then the secondary need not be considered further.

3. TIME PREFILTER

For those secondary satellites which have not been eliminated by the geometrical prefilters, there is yet one more constraint which can be used to remove them from consideration. Even though the elliptical paths may lie within distance D of each other, the two satellites must also simultaneously pass through these regions of closeness in order to have a close encounter between the satellites. This provides the means for a final prefilter based on crossing times for the two satellites of the line of intersection of the two orbital planes.

In general, a satellite will be in a region of vulnerability for a short period of time before and after it flies through the line of intersection of the two orbital planes. An estimate of these times can be obtained analytically by using the perpendicular distance z* from one satellite to the other satellite's orbital plane. Referring to Figure 4 we can see that z* will be less than or equal to r_{rel}. Thus, the times of entry into and exit from the region of vulnerability may be slightly conservative.

The perpendicular distance z* can be determined with spherical trigonometry to be

$$z^* = r \sin I_R \sin u_R. \tag{24}$$

Since we want to find the time when z* = D, we make this substitution in Equation (24) as well as a substitution for r with the help of Equation (14) to obtain

$$D = \frac{a(1 - e^2) \sin I_R \sin u_R}{1 + e \cos(u_R - \omega + \Delta)}, \tag{25}$$

where a is the semimajor axis and e is the eccentricity. Using trigonometric identities, we can write

$$D = \frac{\alpha \sin u_R}{1 + a_x \cos u_R + a_y \sin u_R}, \tag{26}$$

where $\alpha = a(1 - e^2) \sin I_R$ and a_x and a_y were defined in Equations (17). Equation (26) can be solved for $\cos u_R$. After considerable algebra we find

$$\cos u_R = \frac{-D^2 a_x \pm (\alpha - Da_y) Q^{1/2}}{\alpha(\alpha - 2Da_y) + D^2 e^2}, \tag{27}$$

where

$$Q = \alpha(\alpha - 2Da_y) - (1 - e^2) D^2. \tag{28}$$

Now if Q is negative or the right-hand side of Equation (27) has absolute value greater than one, it simply means that the satellite path does not ever get further than D from the other satellite's orbital plane. In such a case, the time prefilter cannot be applied and the satellite must be treated by the coplanar method.

If Equation (27) is determinant for both the primary and secondary satellite orbital elements, we can generate angular windows for each satellite. By taking both values of the arccos in $[0, 2\pi]$ and by using both signs in Equation (27), we obtain the two angular windows

$$[u_R^{(1)}, u_R^{(2)}], \quad [u_R^{(3)}, u_R^{(4)}] \tag{29}$$

as illustrated in Figure 5. The angular windows can be converted to time windows by first using Equation (14) to introduce the true anomaly and then

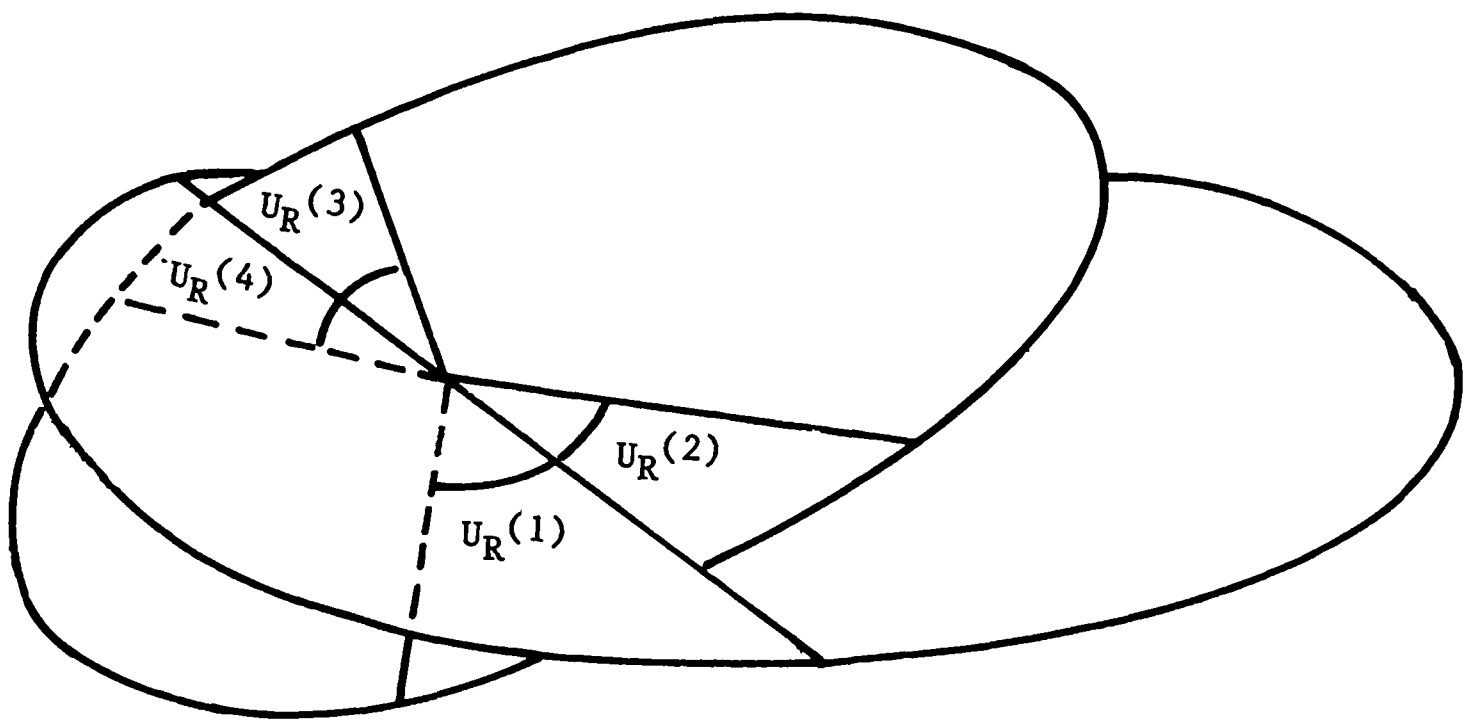

Fig. 5. Angular windows.

using Kepler's equation to convert to mean anomaly and hence to time. The two time windows represent the times of vulnerability for the satellite over a single revolution. By adding multiples of the satellite period to the endpoints of each window, a sequence of time windows can be generated throughout the interval of interest $[t_B, t_E]$. This procedure is followed for both the primary and secondary satellites generating two sequences of time windows. The windows are then cross matched for possible overlapping. Any primary and secondary windows which overlap generate a candidate time calculated as the midpoint of the overlap. These candidate times are used as starting values for an iterative solution of the time of closest approach. This iteration will be discussed in a later section.

The time prefilter will generally eliminate many satellites from further consideration because their orbital motion is out of time phase. For those satellites that it does not eliminate, the interval of interest is usually shortened to a small subset of candidate times by the time prefilter.

4. COPLANAR SATELLITES

For those satellites which are exactly coplanar ($\sin I_R = 0$) or are so near coplanar that the time prefilter cannot be applied, we can generate candidate times for close approaches in the following manner. Recall from Equation (12) that the relative separation distance is

$$r_{rel}^2 = r_p^2 + r_s^2 - 2\underline{r}_p \cdot \underline{r}_s. \tag{30}$$

The time rate of change of this function is given by

$$R = r_p\dot{r}_p + r_s\dot{r}_s - \dot{\underline{r}}_p \cdot \underline{r}_s - \underline{r}_p \cdot \dot{\underline{r}}_s, \tag{31}$$

where we have dropped a common factor of two and where a dot over a variable

denotes its derivative with respect to time. Since R is proportional to the slope of the graph in Figure 1 and since we are looking for relative minima of the graph, we merely start at the beginning of the interval of interest and time step along the primary and secondary orbits searching for a change in sign from negative to positive of the function R in Equation (31). If such a sign change occurs within a step, a candidate for a point of close approach is generated based on linear interpolation. Since we are only searching for a sign change of the function, a large fraction of the orbital period can be used for the time step. In particular, 1/5 of the smaller of the two satellite's periods has proven to be quite adequate.

For those few satellites which fall into the coplanar category, this method provides an efficient way to generate time candidates for points of close approach.

5. POINTS OF CLOSE APPROACH

The candidate times generated either by the time window method or by the coplanar technique are usually quite close to the true times of minima. Hence, they provide very good starting values for a Newton's method solution for the zeros of the function R of Equation (31). The iteration is given by

$$t_{i+1} = t_i - \frac{R}{\dot{R}}, \tag{32}$$

where

$$\dot{R} = \dot{r}_p^2 + r_p\ddot{r}_p + \dot{r}_s^2 + r_s\ddot{r}_s - \ddot{\underline{r}}_p \cdot \underline{r}_s - 2\dot{\underline{r}}_p \cdot \dot{\underline{r}}_s - \underline{\dot{r}}_p \cdot \ddot{\underline{r}}_s. \tag{33}$$

Newton's method for this function is very reliable and converges quite rapidly to give the time of closest approach.

6. PERIODS OF CLOSE PROXIMITY

When two satellites have a close encounter less than D distance, it is of interest to know the beginning and end of the time interval for which they were within D distance of each other (e.g., times t_S, t_F in Figure 1). That is, we seek two zeros of the function

$$H = r_{rel}^2 - D^2 \tag{34}$$

which are in the neighborhood of the minimum point. Since $\dot{H} = 2R$ from Equations (30) and (31), Newton's method gives

$$t_{i+1} = t_i - \frac{H}{2R}. \tag{35}$$

A starting value for the beginning time of close proximity is taken as

a few minutes prior to the minimum time point, and a starting value for the end time of close proximity is taken as a few minutes after the minimum time poirt.

7. MODIFICATIONS FOR PERTURBATIONS

Up to this point the satellites have been assumed to follow two-body orbits in which five of the orbital elements remained constant and the sixth was a linear function of time. In a real world environment, satellite orbits tend to drift secularly away from the two-body state due mainly to the perturbations of the Earth's oblateness and atmospheric drag. The mean effect of these perturbations can be approximated by the equations

$$\begin{aligned} n &= n_0 + \dot{n}_0 t, & \omega &= \omega_0 + \dot{\omega}_0 t, \\ e &= e_0 + \dot{e}_0 t, & \Omega &= \Omega_0 + \dot{\Omega}_0 t, \\ I &= I_0, & M &= M_0 + n_0 t + \dot{M}_0 t + \tfrac{1}{2}\dot{n}_0 t^2, \end{aligned} \tag{36}$$

where n_0 is the mean motion

$$\begin{aligned} \dot{\omega}_0 &= \frac{3}{4} J_2 n_0 \frac{a_e^2}{a_0^2(1 - e_0^2)^2} (5 \cos^2 I_0 - 1), \\ \dot{\Omega}_0 &= -\frac{3}{2} J_2 n_0 \frac{a_e^2}{a_0^2(1 - e_0^2)^2} \cos I_0, \\ \dot{M}_0 &= \frac{3}{4} J_2 n_0 \frac{a_e^2}{a_0^2(1 - e_0^2)^{3/2}} (3 \cos^2 I_0 - 1), \\ \dot{e}_0 &= -\frac{2}{3} \frac{\dot{n}_0}{n_0} (1 - e_0), \end{aligned} \tag{37}$$

and where a_e is the mean equatorial radius of the Earth, J_2 is the coefficient of the second zonal harmonic of the Earth's gravitational field, and $\dot{e}_0$ has been assumed to have such a relationship with $\dot{n}_0$ that the satellite perigee height remains constant as the atmospheric drag circularizes the satellite orbit. The quantity $\dot{n}_0$ is a mean decay rate which is either calculated from an atmospheric model or has been numerically determined from observation of the satellite.

To consider the modifications required to our previous analytical equations, we first assume that both the primary and secondary satellite orbits have been updated in time to the middle of the time span $[t_B, t_E]$ so that the subscript 0 now refers to the middle of the time span of interest. In this way, the impact of the perturbations is lessened by minimizing the time span over which they have to perturb the orbits.

To perform the perigee-apogee prefilter of Equation (1), we first use the first two of Equations (36) to calculate the perigees and apogees of the two satellites at time t_B. Since as we move forward in the time apogee heights decrease and the perigee heights remain constant, we can see that any satellites for which Equation (1) holds at t_B will certainly satisfy this equation throughout the time interval $[t_B, t_E]$.

The effect of the perturbations on the geometrical prefilter is somewhat more complicated. We first calculate the two values of r_{rel}^2 as given by Equation (12) through Equations (23). Note that these two values, d_1 and d_2, will be the minimum geometric distances at time t_{mid}, the midpoint of the span $[t_B, t_E]$. If either of d_1 or d_2 is less than D, the satellite cannot be prefiltered. However, even if both d_1 and d_2 are greater than D, we cannot necessarily eliminate the satellite from consideration, since the perturbation effects will cause d_1 and d_2 to change with time. To account for the time variation, we write

$$r_{rel}^2 = r_{rel}^2{}_{t_{mid}} \pm \left[\frac{d}{dt}(r_{rel}^2)\right]_{t_{mid}} \Delta t, \tag{38}$$

where Δt is half the span length. By using Equation (38) we can predict the secular changes in d_1 and d_2 throughout the time span. If neither d_1 nor d_2 becomes less than D within the time span, then the satellite can confidently be eliminated from consideration. The time rate of change of r_{rel}^2 can be calculated by differentiating Equation (12) to obtain

$$\frac{d}{dt}(r_{rel}^2) = 2r_p\dot{r}_p + 2r_s\dot{r}_s - 2r_p\dot{r}_s \cos\gamma -$$

$$- 2\dot{r}_p r_s \cos\gamma - 2r_p r_s \frac{d}{dt}(\cos\gamma). \tag{39}$$

Using Equation (13) we can write

$$\frac{d}{dt}(r_{rel}^2) = 2\dot{r}_p(r_p - r_s\cos\gamma) + 2\dot{r}_s(r_s - r_p\cos\gamma) -$$

$$- 2r_p r_s[(\cos u_{R_p}\sin u_{R_s}\cos I_R - \sin u_{R_p}\cos u_{R_s})\dot{u}_{R_p} +$$

$$+ (\sin u_{R_p}\cos u_{R_s}\cos I_R - \cos u_{R_p}\sin u_{R_s})\dot{u}_{R_s} -$$

$$- (\sin u_{R_p}\sin u_{R_s}\sin I_R)]. \tag{40}$$

The time rates in Equation (40) can be calculated in a straightforward manner. If we differentiate Equation (11) and use Equation (49) we obtain

$$\dot{I}_R = \sin I_p \sin\Delta_p(\dot{\Omega}_p - \dot{\Omega}_s). \tag{41}$$

The time rates $\dot{r}$ and $\dot{u}$ need to reflect only those secular rates of orbital elements which affect the orbital geometries. Thus, time rates of the mean anomaly which affect in track position can be ignored. Hence,

$$\dot{r} = \frac{r}{a}\dot{a} - a\cos f\dot{e} \tag{42}$$

and from Equation (14)

$$\dot{u}_R = \frac{1}{(1 - e^2)}(2 + e\cos f)\sin f\dot{e} + \dot{\omega}. \tag{43}$$

By using Equations (36) and (37) we can write

$$\dot{r} = \frac{2}{3}\frac{\dot{n}}{n}[a(1 - e)\cos f - r] \tag{44}$$

and

$$\dot{u}_R = -\frac{2}{3}\frac{\dot{n}}{n}\frac{1}{1 + e}(2 + e\cos f)\sin f + \dot{\omega}, \tag{45}$$

where all quantities on the right are to be evaluated at t_{mid}. If we substitute Equations (41), (44), and (45) into Equation (40) and evaluate at t_{mid}, we obtain all necessary quantities for predicting r^2_{rel} over the time span.

By far the most important effect of the perturbations is on the time prefilter. The drag effect causes the period and hence the spacing of windows to change. The oblateness causes the location of the line of intersection of the two orbital planes to drift and hence the point of reference for the windows changes. To take into account the oblateness effects, we divide Equation (9) by Equation (8) to obtain

$$\tan\Delta_p = \frac{\sin I_s \sin(\Omega_p - \Omega_s)}{\sin I_p \cos I_s - \sin I_s \cos I_p \cos(\Omega_p - \Omega_s)}. \tag{46}$$

From Equations (36) we see that the only time dependent quantities on the right-hand side of Equation (46) are Ω_p and Ω_s. If we differentiate Equation (46) with respect to time, we obtain

$$\dot{\Delta}_p = \frac{1}{\sin I_R}\sin I_s \cos\Delta_s(\dot{\Omega}_p - \dot{\Omega}_s), \tag{47}$$

where we have used the spherical trigonometry relation

$$\cos\Delta_s = \cos(\Omega_p - \Omega_s)\cos\Delta_p - \sin(\Omega_p - \Omega_s)\sin\Delta_p\cos I_p. \tag{48}$$

In a similar manner, we can see Equations (10) and (11) to obtain

$$\dot{\Delta}_s = \frac{1}{\sin I_R}\sin I_p \cos\Delta_p(\dot{\Omega}_p - \dot{\Omega}_s). \tag{49}$$

The perturbation effects on the time windows are taken into account by usin the orbital elements at the middle of the span of interest in Equation (27) to calculate the set of time windows nearest the middle of $[t_B, t_E]$. To generate windows earlier or later in time, we must use a satellite period which has been modified to include both the period change due to drag and

the shift of the line of orbital plane intersection due to oblateness. Basically, the next time window will occur when u_R has increased by 2π. The period of time required for this is given by

$$\text{Period} = \frac{2\pi}{\dot{u}_R}. \tag{50}$$

If we ignore periodic variations, then we have the approximation

$$\text{Period} = \frac{2\pi}{n_0 + \dot{M}_0 + \dot{\omega}_0 - \dot{\Delta}_0 + \dot{n}_0 t}. \tag{51}$$

The presence of t on the right-hand side of Equation (51) indicates that the length of the period of u_R is continually changing. However, because we need to add multiples of the period on an incremental basis, we can introduce the following approximation. Let

$$P_{DF} = \frac{2\pi}{n_0 + \dot{M}_0 + \dot{\omega}_0 - \dot{\Delta}_0} \tag{52}$$

be the drag free period (i.e., $\dot{n}_0 = 0$). Then the period after K periods from the reference time (subscript 0) is

$$P_K = \frac{2\pi}{n_0 + \dot{M}_0 + \dot{\omega}_0 - \dot{\Delta}_0 + KP_{DF}\dot{n}_0}. \tag{53}$$

With a little algebra and the binomial theorem, we can approximate Equation (53) by

$$P_K \simeq P_{DF}\left(1 - \frac{2\pi}{n_0}\frac{\dot{n}_0}{n_0} K\right). \tag{54}$$

The modified period of Equation (54) is then used to generate the time windows throughout the span of interest $[t_B, t_E]$.

The modified periods are used for both the primary and secondary satellites to generate sequences of time windows. As before, the window intersections produce time candidates for points of closest approach. All further steps proceed as discussed before with no modifications required.

8. NUMERICAL TESTING

In order to demonstrate the quality and efficiency of the analytical method, we perform some numerical comparisons. Using a historical NORAD (North American Aerospace Defense Command) data base consisting of 4003 satellites, we calculate all approaches with a primary which are closer than 100 km within a one day time span. The primary satellite used has orbital elements

$$n_0 = 14.788 \text{ rev/day},$$

$$e_0 = 0.052,$$

$$I_0 = 82.919°,$$
$$\omega_0 = 110.052°,$$
$$\Omega_0 = 279.648°,$$
$$M_0 = 255.789°,$$
$$\dot{n}_0 = 0.022 \text{ rev/day}^2.$$

We first obtain a truth model by using the brute force stepping technique coupled with the NORAD prediction model to obtain all close approaches less than 100 km within the one day span. By stepping around the orbits searching for a sign change, we identified 102822 possible minimum points. After each of these candidates was refined by iteration, we found only 84 minimum points less than 100 km.

On the other hand, the analytic method produced the following results:

942 satellites prefiltered by perigee-apogee,
1107 satellites prefiltered by geometry.

In all there were 2049 satellites or 51.2% which were eliminated by these two prefilters. Of the remaining satellites, one was near coplanar. The satellites which were not prefiltered have 27280 possible minimum points. Of these, the time window prefilter eliminated 26844 or 98.4% leaving 436 candidates to be considered further. After processing, these candidates produced the same minimum points found by the truth model. On the average, the candidate times generated were within 12 s of the true times of the minimum. Due to the conservative nature of the prefilters and due to some coplanar processing, the analytical method produced 352 extra candidates. On the other hand the brute force technique produced 102738 extra candidates. As expected the analytical method is much more efficient with a computer runtime savings factor of 95 to 1 over the brute force method.

9. CONCLUSION

An analytical method for determining the points of closest approach between satellites has been presented. By using a system of geometrical and time prefilters, the scope of the problem is greatly reduced. Thus, efficiency is improved by two orders of magnitude while retaining reliability and accuracy.

ACKNOWLEDGEMENTS

The analytical method reflects many sources of ideas and inspirations which have evolved in the algorithms used at NORAD over the past 20 years. The

geometrical prefilters and the perturbation formulation are our contribution. However, the exact responsibility for other ideas has been lost to history. Thus, we would like to collectively acknowledge the contribution of NORAD and Ford Aerospace & Communications Corporation personnel.